International Journal of Creative and Open Research in Engineering and Management
ISSN: 3108-1754 (Online)
Volume 02 Issue 09 September-2026 | Impact Factor: 3.5

Spectral-Scale Operators for Battery Digital Twins, Connected Mobility, And Integrity-Gated Quantum Logistics

Gupta AA[1], Shinde S[2]
[1]Research Scholar, [2]Prof, Department of Mathematics
Government College of Engineering, Amravati, Maharashtra, India

How to Cite this Article:

AA, G. (2026). Spectral-Scale Operators for Battery Digital Twins, Connected Mobility, And Integrity-Gated Quantum Logistics. International Journal of Creative and Open Research in Engineering and Management, <i>02</i>(9), 1-9. https://doi.org/10.55041/ijcope.v2i9.113

https://doi.org/10.55041/ijcope.v2i9.113

Abstract—
Operational streams from packs, fleets, and multi-echelon networks arrive as delayed, incomplete, and scale-bearing records rather than as a single smooth series. The paper treats that arrival law as a mathematical fact: time is an oscillatory coordinate, unsigned magnitude is a separate positive coordinate, and sparse marks live in a dual that does not pre-classify events. A mixed product kernel is formed from a two-sided Fourier factor in time and an imaginary-order Macdonald factor on a strictly positive scale. The Fourier coordinate carries oscillation and lag; the KL coordinate carries energy, inventory, payload, and other unsigned magnitudes. Generalized observations are admitted so that switching pulses, theft signatures, demand shocks, and missing telemetry remain distinct until a later classification map is chosen. Quantum annealing is not treated as a front-end estimator. It is placed after spectral consistency, energy feasibility, and provenance checks so that prediction never substitutes for authorization. The same operator language is then used for battery envelopes, mobility cycles, residual twins, and constrained binary dispatch.
The kernel is not offered as an ornamental spectrum. It is the device that keeps lag, unsigned magnitude, and sparse events in distinct slots until a later map is justified. Inversion, when it exists in a chosen weighted space, is treated as a reconstruction of admissible fields rather than as a license to command hardware. The same chart therefore supports pack telemetry, fleet cycles, warehouse flow, and twin residuals without flattening them into one classical oscillator.

Keywords: FKF transform, FKL transform, testing-function space, Macdonald function, distributional transform, sequential convergence, time-shift operator, spectral resonance, digital twin, electric-vehicle battery, smart mobility, supply-chain resilience, blockchain provenance, quantum annealing, QUBO

I. INTRODUCTION

The Electrified fleets and digitally coordinated recovery now generate mixed observations whose time stamps and physical scales do not coincide. Voltage, current, state of charge, temperature, traction power, route motion, inventory, demand, and communication flags occupy different resolutions [34], [16], [11]. Connected mobility adds route and infrastructure coupling [15]. Disturbances in resilient networks travel through several echelons and depend on visibility, recovery stock, and coordination [32], [33], [19]. Digital-twin and AI-logistics reviews frame the same operational setting [5], [6].

Those streams are also incomplete by design: sampling clocks skip, sensors drop, and recovery messages arrive after local buffers have already altered the waveform. A theory that assumes a complete smooth path therefore misstates the object under study. The hybrid construction is written so that incompleteness is a property of the observation, not a defect to be hidden by interpolation [21], [20].

A demand jump is not the same object as a theft pulse, a lost packet, or a slow ageing drift [10]. Smoothing every record into one classical series erases that distinction. The two-sided FKF construction with a Macdonald scale factor keeps temporal oscillation and unsigned magnitude in separate coordinates [27], [26], [21].

Scale mismatch is equally structural. A one-percent inventory swing at a hub is not comparable to a one-percent voltage ripple on a cell string, even when both look like small time-series wiggles. The Macdonald coordinate is reserved for that unsigned magnitude so that resonance tests can name a scale class instead of only a frequency [26], [22].

The aim is to write the mathematical layer first and only then attach applications. Testing-function topology fixes admissible fields [21]. The distributional dual holds impulses [20], [25]. The shift law encodes delay [27], [23]. The transformed residual checks a digital twin [7], [22]. A quantum program is assembled only after those gates close [17], [13], [14].

This order also blocks a common category error in digital operations: using a combinatorial solver as a silent corrector of a bad continuous forecast. Binary search is allowed only on a set already cut by spectral, energetic, and provenance tests [17], [14], [9].

Prediction is therefore not authorization. An estimator may propose a recovery state [8], [29], while a twin reconstructs the field [7] and a ledger records order [9]. Spectral and physical tests stand between that proposal and any binary solver [17], [13]. A later human-centric layer can still withhold the final command [30]. Five sections follow: mixed domain, operators, applications, gated QUBO, and closing remarks.

The introduction therefore ends with a modelling contract. Time carries oscillation and delay; scale carries unsigned physical size; distributions carry marks; residuals carry twin disagreement; QUBO carries only surviving binaries. Later sections do not relax that contract.

2. MIXED TRANSFORM DOMAIN AND TESTING TOPOLOGY

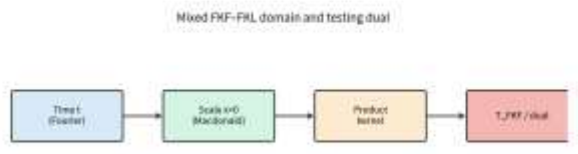

Figure 1. Mixed temporal-scale domain, product kernel, and testing dual used in Section 2.

2.1 Mixed domain and product kernel

The working domain Ω is a half-strip: time is unrestricted while the second coordinate remains strictly positive. Energy, inventory, demand, capacity, distance, and payload are unsigned, so they are not folded into a signed time axis [34], [26].

The half-strip is preferred to a full plane because reflecting x through zero would invent negative energy, negative stock, and negative payload. Boundary behavior as $x \downarrow 0$ is controlled by the Macdonald factor and the testing weights, not by an artificial odd extension [26], [21].

$$\Omega = \mathbb{R}_t \times (0, \infty)_x$$

For an admissible field f(t,x) the mixed transform uses a Fourier factor in t and an imaginary-order Macdonald factor in x [26], [27]. The product kernel therefore reads

Analyticity in the spectral variables is not assumed a priori. What is assumed is that the pairing of kernel against test functions is continuous on T_{FKF}, so the image of a distribution is well defined even when the classical integral diverges [20], [21].

$$K(t, x;\ s, q) = e^{\{-i\, s\, t\}} x^{\{-1\}} K_{\{i\, q\}}\ (x)$$

The resulting image F(s,q) stores oscillation and lag in s while packing magnitude structure in q. FKL calculus governs the scale side; sequential FKF theory governs time and convergence [21], [24]. That split is the first modelling choice of the paper.

A practical corollary is that two records with the same |F| but different arg F differ by lag, whereas two records with similar phase slopes but different q-mass differ by scale. That reading is used unchanged in the battery and multi-echelon sections [27], [23].

2.2 Testing-function topology and sequential convergence

Let T_{FKF} be a testing space whose seminorms control temporal decay, positive-scale growth, and the derivatives required by the kernel [21]. A representative countable family may be written

Seminorms that ignore either time decay or scale growth would admit fields whose transforms are not continuous. The countable family is therefore joint: each index pair (m,n) taxes both sides at once [21].

$$p_{\{m,n\}}(\varphi) = \sup |w_{\{m,n\}}(t, x) \partial_t^m L_x^n\, \varphi(t, x)|$$

Weights and the KL-compatible operator L_x are taken from the sequential-convergence setting of the two-sided transform [21]. Convergence $\varphi_k \to \varphi$ holds when every seminorm of the difference vanishes. Refined telemetry can therefore approach a limit without uniform pointwise control at every sample [20]. The last requirement of this subsection is that the same topology later carry the dual of impulsive events.

Sequential convergence is the operational mode of telemetry refinement. Adding sensors or shortening the sample step should be modellable as a sequence in T_{FKF}, not as a new function space at every firmware release [21], [20].

2.3 Distributional dual

The continuous dual T_{FKF}' admits generalized states. An ordinary field may be augmented by an instantaneous mark through a product of Dirac measures [20], [25]:

Products of Diracs are only the simplest marks. Finite sums of derivatives in t, still supported at a positive scale, represent switching with overshoot and can be kept until a measurement operator is named [25], [20].

$$f = f_{reg} + \alpha\, \delta_{\{t_0\}} \otimes \delta_{\{x_0\}},\ \ x\_0 > 0$$

Switching, theft detection, drop-outs, contacts, and abrupt demand spikes remain sparse until a regularize is applied [10], [28]. The dual therefore refuses to pre-classify a pulse as artefact or shock. That refusal is the operational content of the distributional step.

Classification is postponed because early smoothing would mix a theft pulse with a demand spike and then hand a single “shock” label to the annealer. The dual keeps those marks separate by construction [10], [28].

3. DELAY OPERATORS, DISTRIBUTIONS, AND SPECTRAL RESIDUALS

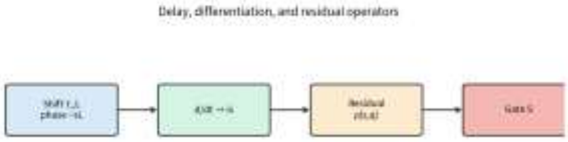

Figure 2. Shift, differentiation, residual concentration, and spectral gate used in Section 3.

3.1 Translation operator and phase law

The temporal translation τ_L acts on time alone and leaves the positive scale fixed [27]. If F denotes the mixed transform,

Scale is frozen under τ_L so that a late truck does not automatically look like a smaller payload. Magnitude invariance of pure delay is the corresponding modulus law [27].

$$F[\tau_L\, f](s,q) \;=\; e^{\{-i\, s\, L\}}\, F[f](s,q)$$

Modulus is invariant under pure delay. If θ(s,q) is an unwrapped phase on a usable band, then Δθ(s,q) = −s L, so the slope in s estimates L [27], [23]. Delay is therefore a spectral phase quantity, while q remains free for scale class [26]. The last sentence of the subsection is that amplitude change and lag are no longer forced to share one diagnostic.

If both lag and amplitude change, the image splits the effects: phase slope for L and q-profile for scale. Joint estimators that ignore that split confound congestion with volume [23], [22].

3.2 Multi-stage delay composition

If a record crosses N stages with lags $L_1, \ldots, L_N$, the composed multiplier is the product of elementary phase factors [27], [23]:

The identity is associative. Grouping stages into corridors or into a single equivalent lag does not change the total phase, which is why downstream observers can still estimate accumulated lead time after aggregation [27], [23].

$$F[\tau_{\{L_1\}} \cdots \tau_{\{L_N\}}\, f](s,q) \;=\; exp(-i\, s \sum_{\{k=1\}}^{\{N\}} L_k\,)\, F[f](s,q)$$

A downstream waveform may be aggregated or buffered and still keep a phase memory of accumulated lead time [32], [33], [19]. Shift-invariant spectral analysis supplies the mechanism [23], [24]. Resilience reading and delay calculus therefore meet in one identity.

Buffering and local control may distort the time waveform while leaving the linear phase law intact on a usable band. That robustness is the reason the shift theorem is treated as an operational instrument rather than as a textbook remark [24], [19].

3.3 Differentiation and transformed dynamics

On test functions or admissible distributions, time differentiation becomes multiplication by the Fourier coordinate [25]:

Higher time derivatives produce polynomials in s. Ageing ramps and slow thermal drift therefore sit at low |s|, whereas switching sits at a broad s-support [25], [16].

$$F[\partial_t\, f](s,q) \;=\; i\, s\, F[f](s,q)$$

A mixed operator A on (t,x) is represented by a multiplier Λ(s,q). Battery, vehicle, and inventory residuals can then be compared in one algebraic chart [34], [16], [22]. The subsection closes by treating Λ as a common response map rather than as a solver.

Comparing Λ across a pack model, a vehicle model, and an inventory model is legitimate only after each model is written as an operator on the same mixed domain [34], [15], [24].

3.4 Distributional continuity and event preservation

If $f_n \to f$ in T_{FKF}, continuity of the transform sends the images to the same limit in the transform topology [21], [20]. Incomplete twin streams may therefore be judged by test-function action instead of by every missing sample [7]. A pulse stays generalized until an explicit smoother G_σ is applied [20]. Preprocessing is not allowed to decide, in advance, whether the mark is theft, switch, artefact, or shock [10]. That veto is the last line of the subsection.

Missing samples are then a statement about which test functions have been paired, not about a hole that must be filled before analysis. Twin residuals inherit that reading [7], [21].

3.5 Spectral residual and resonance functional

Let z_{obs} and z_{twin} be observed and reconstructed fields. Their residual image is weighted by a nonnegative W(s,q) [7], [22]:

The weight W can be tapered near bands that amplify differentiation noise, so the scalar ρ is not dominated by a single ill-conditioned frequency [22], [25].

$$R(s,q) \;=\; W(s,q)|F[z_{obs} \;-\; z_{twin}](s,q)|^2$$

$$\rho \;=\; (\iint\; R\; ds\; dq)\; /\; (\iint\; W\; |F[z_{twin}]|^2\; ds\; dq)$$

A threshold ρ > γ flags a candidate anomaly. Localized peaks are read as multi-scale resonance rather than as a single failure type [22], [24]. Frequency, scale, phase, and support remain available as labels [23], [25]. The subsection ends with that refusal to collapse every amplitude rise into one class.

Resonance here means concentration of residual mass in a localized (s,q) cell, not a mechanical eigenvalue of a chassis. The same word is used because the residue geometry is analogous [22], [24].

3.6 Regularization and stability

Noise may be reduced by a controlled smoother G_σ before transformation [21], [25]. The aim is stability of differentiated bands, not maximal flatness:

Stability of the limit σ→0 is the only license for calling the smooth record a representative of the same generalized state [21].

$$f^{\{\sigma\}} \;=\; G_\sigma \;*\; f, \quad lim_{\{\sigma\to 0\}}\, F[f^{\{\sigma\}}] \;=\; F[f]$$

Provided the topology and kernel allow the limit, smoothing is an explicit operator and not a hidden rewrite of FKF/FKL [26]. Regularization therefore sits inside the theory instead of in front of it.

International Journal of Creative and Open Research in Engineering and Management
ISSN: 3108-1754 (Online)
Volume 02 Issue 09 September-2026 | Impact Factor: 3.5

If the limit fails, the measurement operator has changed the object and must be reported as such. Regularization is therefore an honest map, not a silent rewrite [26].

4. BATTERY, MOBILITY, CHAIN, AND TWIN APPLICATIONS

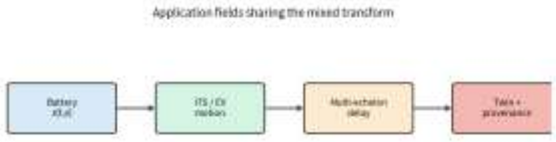

Figure 3. Battery, mobility, multi-echelon, and twin-provenance fields sharing one mixed chart.

4.1 Battery state as a mixed temporal-scale field

Pack states mix electrical, thermal, and ageing coordinates on unlike clocks [34], [16], [31]. A normalized unsigned scale x lets the record be written z(t,x). The hybrid image then splits cycle content from energy-scale content [26].

SoC, temperature, and traction live on unlike clocks, yet they share one unsigned energy scale. Placing that scale on x prevents a thermal spike from being read as a frequency event only [34], [16].

$$z(t,x) = (SoC(t), T(t), P(t);\ x), \quad F_z = F[z]$$

A charging lag L_c multiplies phase by $\exp(-i\, s\, L_c)$, whereas a capacity rescaling moves mass in q [27]. A delayed but consistent trajectory is therefore separable from a trajectory whose envelope has changed [34], [16]. That separation is the closing claim of the subsection.

Mission planning can therefore ask two questions in order: is the trajectory delayed but feasible, or has the envelope itself moved? Only the second question changes pack limits [11], [18].

4.2 Energy feasibility and pack envelope

A spectral flag is not yet a command. Usable energy E_{use} must remain inside pack limits [16], [11], [18]:

Ageing tightens E_{max} over calendar life. A residual peak that would have been feasible on a new pack may violate the tightened envelope and must be rejected before dispatch [16], [31].

$$E_{min} \le E_{use}(t) \le E_{max}$$

A recovery plan is feasible only while the predicted path stays in the pack and ageing envelope [7], [31]. Structural agreement of spectra and physical permission of energy are complementary tests. The subsection ends on that pair of gates.

Complementarity is strict: spectral agreement without energy room is still an illegal command, and energy room without spectral agreement is an unauthorized guess [7].

4.3 Smart mobility and ITS representation

Smart mobility joins motion, routes, sensing, charging sites, and traffic [15]. Velocity v(t) and traction $P_{tr}(t)$ oscillate in s; distance, mass, energy, and power live in q [15], [18]. Two vehicles may share a drive-cycle spectrum and still differ in payload scale [22], [26]. Connected IoT streams occupy the same mixed domain [29], [30]. The last line is that q is the discriminant a purely temporal FFT does not own.

Periodic traffic and inverter switching occupy s; gross vehicle mass and stored energy occupy q. A light urban cycle and a loaded intercity cycle can share harmonics and still separate in q [15], [18].

4.4 Multi-echelon supply-chain dynamics

Let $D_k(t, x)$ be flow at echelon k. A stage lag L_k contributes a phase factor, and after N stages the accumulated delay sits in arg F [27], [23]. Magnitude, inventory, and capacity remain on the scale axis. Delay propagation is therefore not confused with scale amplification [32], [33], [19]. Resilience studies inherit that split as a measurable distinction.

Bullwhip-like amplification appears as growth of q-mass along the chain, whereas added lead time appears as phase. Those two signatures recommend different recovery tools [32], [23].

4.5 Digital-twin residual architecture

The twin may be physics-based, data-driven, or hybrid [7], [8]. The consistency gate admits a prediction only when $\rho \le \gamma$ [8], [29]. An AI forecast can be informative and still unauthorized until the residual test passes [7], [22], [9]. The operator, not the predictor, owns the last word of the subsection.

Hybrid twins are allowed, but the residual test does not inspect the training recipe. It only inspects whether the reconstructed field is spectrally close to the observation [7], [8].

4.6 Blockchain provenance as an independent constraint

Let h_k be a provenance state on an ordered telemetry list [9]. A decision needs both spectral evidence and a traceable chain [9], [29]. A ledger shows origin; it does not prove pack feasibility [7], [33]. Interface pulses, including anti-theft marks, stay distributional until classified [10], [12]. Provenance and physics therefore remain separate constraints.

A broken hash sequence vetoes the record even if ρ is small. Conversely, a perfect ledger with a large residual still fails the twin test [9], [7].

4.7 Resilience decision space

The admissible action set joins residual, provenance, and envelope tests [32], [19]:

A is not a utility. It is a constraint set. Optimization is forbidden on its complement, however attractive the nominal cost [32], [14].

$$A = \{\, a \mid \rho(a) \le \gamma, P(a) = 1, E(a) \in [E_{min}, E_{max}] \,\}$$

Actions outside A never reach the combinatorial layer. Resilience is then reaction inside a validated set, not mere speed [7], [30], [33]. That definition closes the application section.

That veto is the operational meaning of integrity-gated logistics: speed is allowed only after the state has been validated [30], [33].

5. INTEGRITY-GATED QUANTUM DECISION ARCHITECTURE

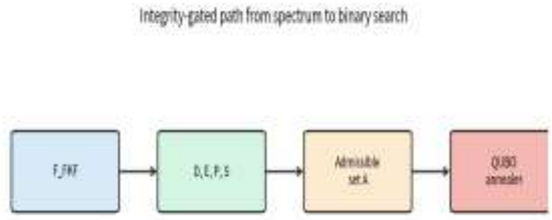

Figure 4. Spectral, physical, and provenance gates placed upstream of QUBO annealing.

5.1 Separation of state estimation and binary optimization

Quantum logistics tasks include assignment, placement, recovery choice, and unit-load layout [17], [13], [14]. Those bits must be kept apart from continuous energy, temperature, inventory, and residuals. If $y_j \in \{0,1\}$, the continuous state defines the region and y only selects a pattern inside it [14], [29]. A solver is not allowed to repair an invalid physical forecast [16], [11].

Continuous estimation and binary search therefore use different mathematical objects. Confusing them lets an annealer invent energy that the pack does not hold [16], [11].

5.2 QUBO construction

Operational cost C(y) is completed by nonnegative quadratic penalties [14], [13]:

Equality constraints become squares; inequalities become slack bits or barrier penalties. Either route must remain quadratic after expansion [14], [13].

$$Q(y) = C(y) + \sum_{\ell} \lambda_{\ell} \left(\sum_{j} a_{\{\ell j\}}\, y_j - b_{\ell} \right)^2$$

Because each y_j is binary, squares expand into linear and pairwise terms suited to annealing [17]. Penalty weights must be large enough to block infeasible vertices without erasing cost gaps among feasible ones. That calibration is the last modelling remark of the subsection.

If penalties overwhelm C, the annealer reports feasibility and hides cost. If they are too small, it reports cost and hides feasibility. Both failures are classical modelling errors, not quantum errors [17].

5.3 Energy-aware logistics optimization

Pack and vehicle limits enter the QUBO only after continuous feasibility is checked [34], [16], [15]. For route r,

Reserve E_{res} is a policy number, not a spectral output. It is attached after ρ and provenance have already passed [16], [19].

$$E_{req}(r) + E_{res} \leq E_{use}$$

A violating route is excluded or heavily penalized before annealing. Thermal limits, charge access, and payload bounds are treated the same way [16], [18]. Energy is therefore a pre-filter, not an afterthought inside the annealer.

Exclusion is preferred to a mild penalty when the violation is physical rather than economic [15], [18].

5.4 Spectral preconditioning of recovery decisions

The residual map yields a disturbance score Φ_j for each binary option [22], [24]. Base costs become $c_j + \kappa \Phi_j$. The quantum device does not diagnose spectra; the classical layer only tilts the landscape [23], [25]. The annealer then searches under constraints inherited from the validated state [14], [13]. Preconditioning remains outside the chip.

κ is chosen so that Φ_j reorders nearby feasible options without resurrecting options already removed from A [22], [24].

5.5 ULD and disruption configuration

Unit-load binaries may encode slot assignment, recovery pick, or placement [14]. Payload, volume, geometry, centre of gravity, adjacency, stacking, and structure stay distinct from spectral diagnosis. FKF/FKL preconditioning asks whether the disruption and its delay path justify a scenario [27], [23], [24]. QUBO then selects one efficient feasible layout [14], [29]. Diagnosis and packing therefore keep separate jobs.

Geometry and centre-of-gravity constraints are classical and remain classical. The transform only decides whether the disruption narrative that motivates a reload is spectrally supported [27], [23].

5.6 Prediction is not authorization

The decision chain is a composition of operators. F_FKF writes the mixed image [27], [21], [26]; D tests the twin [7]; E tests energy [34], [16]; P tests provenance [9]; S tests spectral admissibility [22], [24]. Only the surviving set reaches a binary solver [17], [14].

Composition is written left to right as authorization depth: spectrum, twin, energy, provenance, residual gate, then search [27], [7], [9].

Industry 5.0 reading places a human stop after search [30]. A predictor may name a likely state [8]; the transform tests consistency [21], [20]; physics may reject the path [34], [11]; a ledger traces the record [9]; annealing ranks the rest [13], [14]. Final operational control can still be withheld [30], [29].

Human veto is outside A and outside Q. It is a final operational control, not a substitute for the mathematical gates [30], [29].

5.7 Integrated architecture and research implications

Battery work supplies energy states [34], [16], [18]. Mobility work supplies connected traces [15], [29]. Spectral papers supply resonance diagnostics [22], [24], [25]. AI, ledgers, and twins supply forecast, order, and reconstruction [7], [8], [9]. Resilience work supplies the recovery objective [32], [33], [19]. Quantum papers supply combinatorial search [17], [13], [14]. FKF/FKL papers supply the backbone [27], [21], [20].

The pipeline is therefore both an operator chain and a literature map: energy papers feed E, spectral papers feed S, and ledger papers feed P [34], [22], [9].
The order blocks three category errors. A large forecast is not a feasible pack state. An integrity pulse is not a demand shock [10], [20]. A cheap binary vector is not a valid operation [14], [13]. The mathematical gate keeps those distinctions before optimization [24], [30].
Future numerical work should report all three error rates separately: false physical authorization, false shock classification, and false cheap binaries. A single aggregate accuracy score would hide the gates that this architecture exists to protect [24], [20].

CONCLUSION

A mixed Fourier–Macdonald kernel was used as a common language for delayed, unsigned-scale, and impulsive records. Testing topology, distributional dual, phase delay, and weighted residuals form a gate in front of any binary program. Battery envelopes, mobility cycles, multi-echelon lags, twin residuals, and provenance flags occupy that same chart without being forced into one smooth series.
The construction does not claim that one transform replaces battery management, traffic control, or warehouse software. It claims that those systems can share a typed language for delay, scale, marks, and residuals before any of them is allowed to write a binary command.
Artificial intelligence remains a proposal engine; the twin remains a consistency engine; the ledger remains an evidence engine; annealing remains a search engine over an already restricted set. Future work should sharpen inversion and stability on weighted testing spaces, measure missing-data bias, build fractional or adaptive kernels, and trial the spectral-to-QUBO interface on packed, fleet, and multi-echelon archives.
Until those checks exist on packed cells, instrumented corridors, and multi-echelon ledgers, the architecture should be read as a contract on the order of operators rather than as a finished controller. The contract is the contribution.

REFERENCES

[1] S. M. Harle et al., "Artificial Intelligence Approaches for Strength Prediction and Optimization of Composite Concrete Mixtures: A Systematic Review and Future Research Framework," International Research Journal of Modernization in Engineering Technology and Science, Vol. 8, pp. 81–97, July 2026.

[2] S. M. Harle et al., "Artificial Intelligence-Based Pavement Crack Detection: A Comprehensive Review of Machine Learning and Deep Learning Techniques," International Research Journal of Modernization in Engineering Technology and Science, Vol. 8, pp. 50–69, July 2026.

[3] S. M. Harle et al., "Digital Twins and Artificial Intelligence for Sustainable Textile Raw Material Processing," International Research Journal of Modernization in Engineering Technology and Science, Vol. 8, pp. 14–30, July 2026.

[4] Harle SM, "Investigation of Mechanical Behavior of Steel Fiber-Reinforced Geopolymer Concrete Under ulti-Axial Stress Conditions," Hydraulic and Civil Engineering Technology IX: Proceedings of the 9th International Technical Conference on Frontiers of HCET, Sanya, China, SAGE Publications, 25-27 Sept pp 555-561 , 2024

[5] Akarshan Gulhane, "Digital Twin Technology for Building Resilient and Adaptive Global Supply Chains: A Review," International Research Journal of Modernization in Engineering Technology and Science, Vol. 6, Issue 12, 2024. DOI: 10.56726/IRJMETS64992.

[6] Akarshan Gulhane, "Artificial Intelligence Applications in Sustainable Logistics and Green Supply Chain Management: A Bibliometric Review," International Research Journal of Modernization in Engineering Technology and Science, Vol. 6, Issue 12, 2024. DOI: 10.56726/IRJMETS65006.

[7] Akarshan Gulhane, "Artificial Intelligence and Blockchain Integration for Enhancing Supply Chain Transparency, Traceability, and Resilience," International Research Journal of Modernization in Engineering Technology and Science, Vol. 6, Issue 12, 2024. DOI: 10.56726/IRJMETS65016.

[8] Akarshan Gulhane, "Power Line Carrier Communication Based Anti-Theft System," International Journal of Research in IT and Management (IJRIM), Vol. 4, Issue 12, pp. 1–11, 2014.

[9] Akarshan Gulhane, "Battery Sizing for Plug-in Hybrid Electric Vehicles — Formula Hybrid," IEEE International Conference on Power, Control, Signals and Instrumentation Engineering (ICPCSI), pp. 368–372, 2017. DOI: 10.1109/ICPCSI.2017.8392317.

[10] Gulhane, A. (2014). Swipe Controller. International Journal of Research in Engineering and Applied Sciences (IJREAS), 4(12), 1–7.

[11] Akarshan Gulhane, "Navigating the Quantum Revolution in Logistics: Opportunities and Practical Applications in Supply Chain Management," International Journal of Engineering and Techniques (IJET), Vol. 12, pp. 553–556, 2026. DOI: 10.29126/ijet.2026.v12.i3.553 [1, 2]12

[12] Akarshan Gulhane, "Quantum Computing for

Logistics Optimization: Annealing in Unit Load Device Configuration and Disruption," International Journal of Research Publication and Reviews, Vol. 7, Issue 6, pp. 4643–4648, June 2026. DOI: 10.55248/gengpi.07.0626.16a57.

[13] Akarshan Gulhane, "Smart Mobility and Intelligent Transportation Systems: Emerging Trends, Technologies, and Challenges," International Journal of Scientific Research in Engineering and Management (IJSREM), Vol. 9, Issue 11, Nov. 2025. DOI: 10.55041/IJSREM53436.

[14] Akarshan Gulhane, "Recent Advances in Electric Vehicle Battery Technologies: Materials, Management Systems, and Sustainability Perspectives," International Journal of Scientific Research in Engineering and Management (IJSREM), Vol. 9, Issue 7, Jul. 2025. DOI: 10.55041/IJSREM51198.

[15] Akarshan Gulhane, "Quantum Computing in Transportation and Logistics: Current State, Industrial Applications, and Future Directions," International Journal of Scientific Research in Engineering and Management (IJSREM), Vol. 9, Issue 9, Sep. 2025. DOI: 10.55041/IJSREM52469.

[16] Akarshan Gulhane, "Solar-Assisted Electric Mobility: Design Framework and Performance Assessment of Sustainable Hybrid Vehicle Architectures," Int. J. Engg. Res. & Sci. & Tech., Vol. 21, No. 3, pp. 362–368, 2025. DOI: 10.56636/ijerst.2025.v21.i03.3594.

[17] Akarshan Gulhane, "Supply Chain Resilience in the Era of Digital Transformation: A Systematic Literature Review and Research Agenda," Int. J. Engg. Res. & Sci. & Tech., Vol. 21, No. 4, pp. 1058–1068, 2025. DOI: 10.56636/ijerst.2025.v21.i04.3812.

[18] Akarshan Gulhane, "Distributional Extension of the FKF Transform and Its Relevance to Supply-Chain Systems," International Journal of Creative and Open Research in Engineering and Management ISSN: 3108-1754 (Online) Volume 02 Issue 08 August 2026 , DOI: https://doi.org/10.55041/ijcope.v2i8.137

[19] Akarshan Gulhane, "Sequential Convergence in the Testing Function Space of the Two-Sided FKF Transform," International Journal of Creative and Open Research in Engineering and Management ISSN: 3108-1754 (Online) Volume 02 Issue 08 August 2026, DOI: https://doi.org/10.55041/ijcope.v2i8.138

[20] Akarshan Gulhane, " Spectral Analysis for Multi Scale Supply Chain Dynamics and ResidueBased Resonance Extraction in Hybrid-Vehicle Systems," International Journal of Creative and Open Research in Engineering and Management ISSN: 3108-1754 (Online) Volume 02 Issue 08 August 2026, DOI: https://doi.org/10.55041/ijcope.v2i8.141

[21] Akarshan Gulhane, " Shift-Invariant Spectral Analysis of Multi-Echelon Supply-Chain Lead Times via the FKF Transform," International Journal of Creative and Open Research in Engineering and Management ISSN: 3108-1754 (Online) Volume 02 Issue 08 August 2026, DOI: https://doi.org/10.55041/ijcope.v2i8.136

[22] Akarshan Gulhane, " Spectral Framework Based on the FKF Transform for Supply Chain Dynamics and Resilience," International Journal of Creative and Open Research in Engineering and Management ISSN: 3108-1754 (Online) Volume 02 Issue 08 August 2026, DOI: https://doi.org/10.55041/ijcope.v2i8.140

[23] Akarshan Gulhane, " Spectral Differential Properties of the Distributional FKF Transform with Applications to Resilient Supply-Chain Systems," International Journal of Creative and Open Research in Engineering and Management ISSN: 3108-1754 (Online) Volume 02 Issue 08 August 2026, DOI: https://doi.org/10.55041/ijcope.v2i8.139

[24] Akarshan Gulhane, " FKL Transform Key Properties, And Applications To Supply-chain Analysis," International journal of Engineering sciences and Advanced Technology, Published:11-12-2025, Issue: Vol. 25 No. 12 (2025), Page Nos: 596-605, DOI: https://doi.org/10.64771/ijesat.2025.v25.i12.3816

[25] Akarshan Gulhane, " Expanded Treatment Of The Time-Shift Property Of FKF Transform With Supply-Chain Applications," International journal of Engineering sciences and Advanced Technology, Published:11-12-2025, Issue: Vol. 25 No. 12 (2025), Page Nos: 606 – 616, DOI: https://doi.org/10.64771/ijesat.2025.v25.i12.3817

[26] Akarshan Gulhane, " The FKF Transform: Exponential Modulation Properties And Applications To Secure Digital Supply-Chain Networks," International journal of Engineering sciences and Advanced Technology, Published:11-12-2025, Issue: Vol. 25 No. 12 (2025), Page Nos: 617 – 623, DOI: https://doi.org/10.64771/ijesat.2025.v25.i12.3818

[27] Akarshan Gulhane, "Internet of Things, Artificial Intelligence, and Quantum Computing: A Convergent Framework for Smart Logistics Ecosystems," International Journal of Engineering Science and Advanced Technology (IJESAT), Vol. 24, Issue 12, pp. 297–317, 2024. DOI:

10.64771/ijesat.2024.v24.i12.3372

[28] Akarshan Gulhane, “Industry 5.0 and Intelligent Logistics: Transforming Supply Chain Operations through Human-Centric Automation,” International Journal of Engineering Science and Advanced Technology (IJESAT), Vol. 24, Issue 12, pp. 287–296, 2024. DOI: 10.64771/ijesat.2024.v24.i12.3371

[29] Akarshan Gulhane, “The Future of Vehicles: Solar-Powered Battery Electric Hybrid Vehicle Architecture,” Tech Briefs Contest, 2020.

[30] Akarshan Gulhane, “A review of resilience in global supply chains,” International Engineering Journal for Research & Development, vol. 8, no. 4, 2024.

[31] Akarshan Gulhane, “Weaving resilience: Navigating internal and external complexities in modern supply chains,” International Journal of Ingenious Research, Invention and Development, vol. 3, no. 1, pp. 123–128, 2024, doi: 10.5281/zenodo.11491482.

[32] Akarshan Gulhane, “Advancements in automotive batteries: A review,” International Engineering Journal for Research & Development, vol. 8, no. 6, pp. 18–57, 2023. [Online]. Available: https://iejrd.com/index.php/iejrd/article/view/3141

[33] Ivanov, D., Dolgui, A., & Sokolov, B. (2019). The impact of digital technology and Industry 4.0 on the ripple effect and supply chain risk analytics. International Journal of Production Research, 57(3), 829–846.

[34] Ivanov, D. (2021). Digital supply chain twins: Managing the ripple effect, resilience, and disruption risks by data-driven optimization, simulation, and visibility. In Handbook of Ripple Effects in the Supply Chain (pp. 309–330). Springer.